



Kinetic, equilibrium and thermodynamic studies of synthetic dye removal using plastic waste activated carbon prepared by CO₂ activation

T.K.Manimekalai¹, G.Tamilarasan², N.Sivakumar^{2*} & S.Periyasamy³

¹Department of chemistry, J. K. K. Munirajah College of Technology, T.N.Palayam, Gobi, Erode-638506, India

²Department of Chemistry, Chikkanna Government Arts and Science College, Tirupur-641602, India

³Department of Textile Technology, PSG College of Technology, Coimbatore-641004, India

Abstract: Activated carbon prepared by CO₂ activation of pyrolysed chars of waste plastic materials used as a high-efficiency adsorbent for the removal of a reactive dye from textile industrial effluents. Characterizations of the synthesized plastic waste activated carbon (PWAC) were analyzed using SEM, XRD and FTIR analysis. The effects of temperature, initial concentration, and contact time were systematically investigated. The equilibrium adsorption data fitted the Langmuir isotherm well and the monolayer adsorption capacity was 68.21 mg/g. Moreover, kinetics of adsorption exhibit followed the pseudo-second-order kinetic model. Thermodynamic parameters such as Gibbs free energy, enthalpy and entropy were determined. It was found that reactive dye adsorption was spontaneous, exothermic and physisorption process.

Keywords: Plastic waste activated carbon; Adsorption; Reactive blue; Isotherm; Kinetics; Thermodynamics.

1. Introduction

In a global point of view the disposal of waste water discharged from the textile, printing, plastics and tanning industries is a major problem for water pollution. Textile industries are produces a huge amount of wastewater, which contains toxic, mutagenic carcinogenic substances which generate the severe threats to aquatic creature, animals and human health [1]. It is estimated that more or less 12% of synthetic dyes are lost during manufacturing and operating process and 20% dyes lost penetrate the industrial wastewaters [2]. Synthetic dyes are eliminated from textile industrial effluents under aerobic treated conditions; they are almost decomposed into aromatic amines under anaerobic degradation condition [3]. Large numbers of reactive dyes are azo compounds and also these are highly soluble in water, it is difficult to remove the dyes using chemical coagulation [4]. Adsorption process has been renowned as a potential method due to its ease of operation, simple design, high efficiency and low cost of application. In the past few decades the production consumption of the thermoplastics such as polyethylene (PE), polypropylene (PP), polystyrene (PS), polyethylene terephthalate (PET) and polyvinylchloride (PVC) recorded fastest growth rate in the world plastic market. It was reported that the world production of plastics increased from 1.7 million tons in 1950 to 288 million tons in 2012 [5]. It has been estimated that almost 60% of plastic solid waste is discarded in open space or land filled worldwide [6]. Plastics waste are among the major and most challenging sources of solid wastes.

Traditional methods for the treatment of waste plastics are landfill and incineration, which causes the environmental pollution. Pyrolysis of waste plastic mixture is a potential way of conversion of waste plastic into low-emissive hydrocarbon fuel oil, fuel gas and char an additional product is obtained, which could be upgraded to produce activated carbon for adsorption of textile effluents, heavy metals and used as a solid fuel [7-10].

In this study, plastic waste activated carbon (PWAC) was utilized as a novel adsorbent for removal of a reactive blue 2 dye from aqueous solution. We examined the effects of contact time, initial dye concentration and temperature on reactive blue 2 adsorption processes onto PWAC from textile industrial effluents. FT-IR analysis was carried out to understand the surface functional groups on the adsorbent. Equilibrium data were analyzed by six different equilibrium isotherm models. Kinetic data were evaluated by pseudo-first order, pseudo-second order, Elovich and Intraparticle diffusion models. Thermodynamic parameters such as free energy (ΔG), enthalpy (ΔH) and entropy (ΔS) were also determined to understand the spontaneity of the adsorption process.

2. Materials and Methods

2.1. Preparation of the adsorbent (PWAC)

The plastic mixture used for the experiment which comprises 38% of polyethyleneterephthalate (PET), 38% of polyvinyl chloride (PVC), 19% polypropylene (PP) and 5% HZSM-5 (catalyst was obtained from a Sud-Chemie India Pvt. Ltd) were placed in tubular reactor and heated at $10^\circ\text{C min}^{-1}$ to 600°C for 1h in N_2 atmosphere. 10% carbon yield was obtained after the pyrolysis and residues were powdered with mortar and then washed with 200 ml of concentrated hydrochloric acid using magnetic stirrer for 1h to remove the inorganic impurities. Finally the residue was rinsed with distilled water until the filtrate's p^{H} becomes 7. The final char was dried in a hot air oven at 100°C and it was left to cool over-night. The final activation of char carried out in a specially designed stainless steel reactor at 900°C in the presence of CO_2 .

2.2. Preparation of adsorbate

An anionic dye (Reactive Blue 2) having molecular formula $\text{C}_{29}\text{H}_{17}\text{ClN}_7\text{Na}_3\text{O}_{11}\text{S}_3$, MW: 840.11g/mol, CI No. 61211 and λ_{max} -604 nm was chosen as an adsorbate. A stock solution containing 1 gm of dye per litre was prepared by using distilled water and was used to prepare the adsorbate solutions by appropriate dilution as required. The pH of dye solutions was adjusted with 0.01M NaOH and 0.01M HCl using a pH meter.

2.3 Error Analysis

To govern the validity of isotherm, kinetics models and statistical analysis was carried out. In all regression cases, three different error functions, i.e., the sum of the square of the error (SSE), Root mean square error (RMSE) and chi-square between the experimental data and calculated values were evaluated using the following equations [11-12];

$$RMSE = \sqrt{\frac{1}{N-2} \sum_{i=1}^n (q_{e,exp} - q_{e,cal})^2}$$

$$\chi^2 = \sum_{i=1}^n \frac{(q_{e,exp} - q_{e,cal})^2}{q_{e,exp}}$$

$$SSE = \sum_{i=1}^n (q_{e,cal} - q_{e,exp})^2$$

Where $q_{e,exp}$ and $q_{e,cal}$ are the experimental and calculated adsorption capacity (mg g^{-1}) and n is the number of measurements.

3. Results and discussions

3.1. Characterization of adsorbent

The Morphological characteristics of the samples were studied using JSM-5610LV Scanning Electron

Microscope (SEM). The phase structures of PWAC were analysed by X-ray diffraction (XRD) using a PANalytical advance X-ray diffractometer with Cu $K\alpha$ radiation operating at 40 kV and 30 mA. Fourier Transform Infrared (FT-IR) measurements were carried out using Shimadzu instrument.

3.2. Scanning Electron Microscope analysis

The surface morphology of plastic waste unactivated and activated carbon is given in Fig. 1a & 1b. The unactivated sample particles are compacted tightly and uniformly distributed and does not showed more open porous structures. The activated sample showed that the activation stage produced extensive external surfaces with quite irregular cavities and pores. The inner carbonaceous phase also becomes fragmented, indicating that the carbon skeleton is severely broken and a “loose sponge” structure is formed during the activating process. The surface of PWAC looks much smoother and pores are arranged irregularly. Small pores can be seen on the inner waals of larger pores and it was making difficult to determine individual particle size by SEM [13].

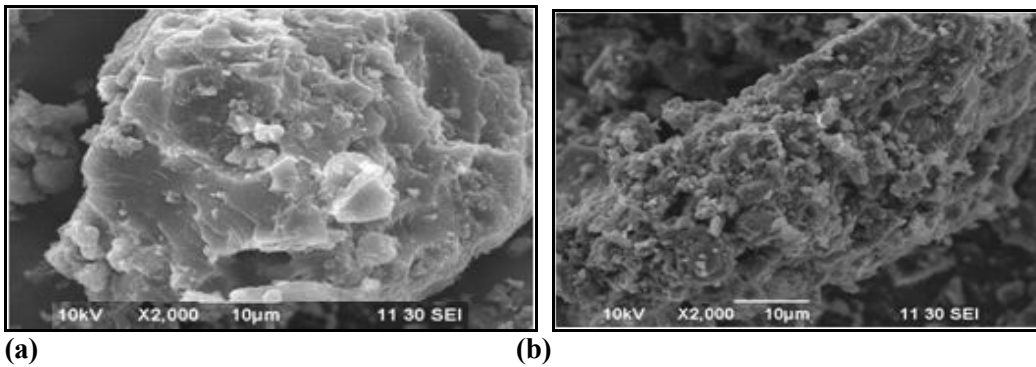


Fig. 1. SEM image of a) Plastic waste unactivated carbon, b) PWAC

3.3. FTIR Analysis

The FTIR spectroscopic study of the raw carbon and plastic waste activated carbon are shown in Fig. 2a, and b. Oxygen containing surface functional groups plays a very important role in the adsorption process and initiates a chemical bonding between adsorbent and adsorbate species. A peak between 3743.83 and 3417.86 cm^{-1} was observed from the FT-IR spectra of unactivated and activated sample of solid plastic waste mixture, which can be ascribed to the $-\text{OH}$ stretch of hydroxyl functional group. The peak observed at 1514.12 , 1541.12 and 1220.94 cm^{-1} are related to the $\text{C}-\text{H}$ stretching of alkane, the $\text{C}=\text{C}$ stretching of thearomatics and the $\text{C}-\text{O}-\text{C}$ stretching vibration of the esters, ether and phenol groups of the activated sample. The $\text{C}-\text{O}$ stretching or $-\text{OH}$ deformation band in carboxylic acid was observed at 1421.54 cm^{-1} of the unactivated sample. The band at 1093.64 cm^{-1} could also be assigned to alcohol ($\text{R}-\text{OH}$) groups. The peaks found at 798.53 cm^{-1} is due to $\text{Si}-\text{O}$ or $\text{C}-\text{O}$ stretching in alcohol, ether or hydroxyl groups, $\text{Si}-\text{H}$ groups. The adsorption band region 621.08 cm^{-1} ascribed to $\text{C}=\text{O}$ out of plane band of $\text{Si}-\text{O}$ bending vibrations contributing to the strong absorptions in the $400-600\text{ cm}^{-1}$ region observed both activated and unactivated carbon sample [14]. After activation of the plastic waste carbon sample by using CO_2 , some of peaks shifted their frequency level or, in some cases, disappeared. A similar phenomenon has been observed [15] and reported that different oxygen groups, which were present in the raw pistachio nut shell, disappeared after the heat treatment, causing the aromatization of the carbon structure.

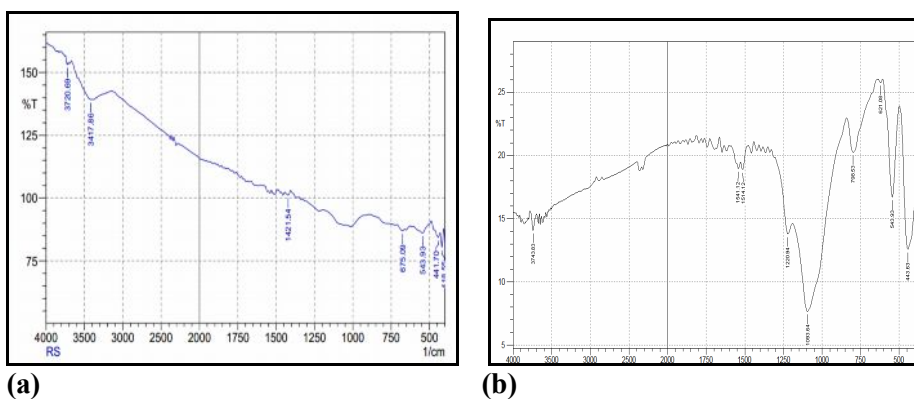


Fig. 2. FT-IR Spectra of a) Plastic waste unactivated carbon b) PWAC

3.4. XRD Analysis of PWAC

The X-ray pattern can be used to confirm that the sample being analyzed is amorphous or crystalline. Amorphous materials do not have long range order like crystalline materials and therefore the resulting diffraction pattern show the typical series of peaks associated with crystalline materials. The diffraction pattern of materials shows a broad “halo” with few or single maxima, Fig. 3. Although this “halo” pattern uniquely identify the material being studied it confirm that the material is crystalline, which is critical knowledge needed for characterization. While, powder X-ray diffraction is used to identify and monitor the crystalline solid form of the active ingredient in a small molecule formulation of excipient form an amorphous or crystalline matrix [16].

The literature of carbon materials repeatedly refers to the crystallite and to the crystallite size, with its graphitic connotations, in analyses of structure within activated carbon based on XRD data. The XRD diagrams of activated carbon prepared from polymeric waste indicate the intense main peak shows the presence of highly organized crystalline structure of activated carbon. These crystalline structures of PWAC, new diffraction peaks appeared indicating that there was a change in chemical composition of crystals frame work as new species formed as a result of activation. From the unactivated to activate sample, the decreases in peak intensities were marginal which indicated a fairly intact crystal structure owing of activation process. Adsorption of dyes onto prepared activated carbon, where the dyes adsorbed on the upper layer of the crystalline structure of the carbon surface by means of physisorption [17].

The strong diffraction peak emerged at $2\theta = 22- 25^\circ$ and $2\theta = 45.44^\circ$ peaks indicates the existence of graphite crystallite in both carbon materials [18]. It is generally expected that increasing the pre-carbonization temperature promotes the growth of the graphitic micro-crystallites and sharpens at XRD peaks of the produced activated carbon [19]. The diffraction peak at $2\theta = 7.72^\circ$ and 8.66° peak of PWAC indicates HZSM-5 catalyst structure [20]. The both carbon material mainly showed two diffraction peaks; one at $2\theta = 24-26^\circ$ and other at $2\theta = 43-45^\circ$ due to graphitic planes. The intensity and base area of peaks depends upon the crystallinity of carbon materials. The XRD result showed that $2\theta = 14-19^\circ$ indicates SiC and $2\theta = 45-46^\circ$ indicates SiO₂ have a fine structure, owing to the presence of catalyst HZSM-5 [21].

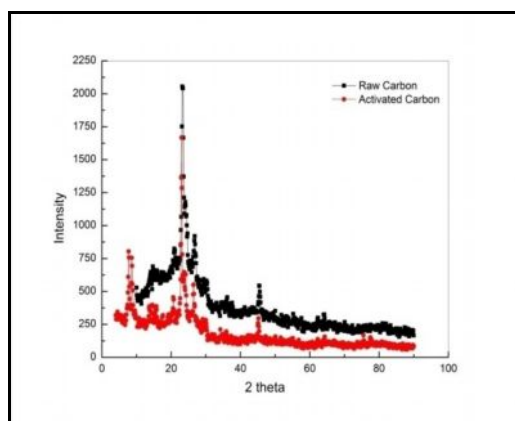


Fig.3. XRD analysis of PWAC

3.5. Adsorption Isotherm Studies

The simplest method for determination of the isotherm constants for two parameter isotherms is to linearize the model equation and then apply linear regression. The equilibrium measurements were focused on the determination of the adsorption isotherms. The relationship between the amounts of adsorbed dye per unit mass of the plastic waste adsorbent (q_e) and the equilibrium solution dye concentration (C_e) for the temperature range of 30-60 °C. It was found that the adsorption capacity increased as the temperature was increased from 30 °C to 60 °C.

Isotherm data should be accurately fit to a suitable isotherm model to find adsorption parameters that can be used in a single batch design process [22]. There are several isotherm equations available for analyzing experimental sorption equilibrium data in single-solute systems. The most commonly used are the Langmuir, Freundlich, Temkin, D-R, Halsey and Jovanovic models.

3.5.1. Langmuir isotherm

The Langmuir adsorption isotherm is based on the assumption that all sites possess equal affinity for the adsorbate. It may be represented in the linear form as follows [23].

$$\frac{C_e}{q_e} = \frac{1}{K_L Q_m} + \frac{C_e}{Q_m}$$

Where Q_m is the maximum reactive blue 2 uptake, mg/g, K_L the Langmuir adsorption constant, L/mg. The model provides the maximum values where they could not be reached in the experiments. The values of K_L were decreased with increasing temperature of the studied system. The K_L values indicate adsorption affinity. The monolayer saturation capacity, Q_m , were 68.21, 64.78 and 59.83 mg/L for PWAC at different temperature respectively. From Table 1 it can be observed that the calculated isotherm parameters and their corresponding RMSE, SSE and χ^2 values vary for the six linearized types of isotherm models. It can be seen that the Langmuir model yields a better fit than the Freundlich, Temkin model and other isotherm models, as reflected by a RMSE, and χ^2 values. Langmuir isotherm showed better fit followed by Temkin isotherm model in terms of coefficient determination values.

The essential feature of the Langmuir isotherm can be expressed by means of R_L ($R_L=1/1+bC_0$), a dimensionless constant referred to as separation factor or equilibrium parameter.

The value of R_L indicated the type of isotherm to be irreversible ($R_L=0$), favourable ($0<R_L<1$), linear ($R_L=1$) or unfavourable ($R_L>1$). Further, the R_L value for Reactive blue 2 onto PWAC at 30 to 60°C are 0.0529 to 0.656 indicates adsorption process is favourable[24]

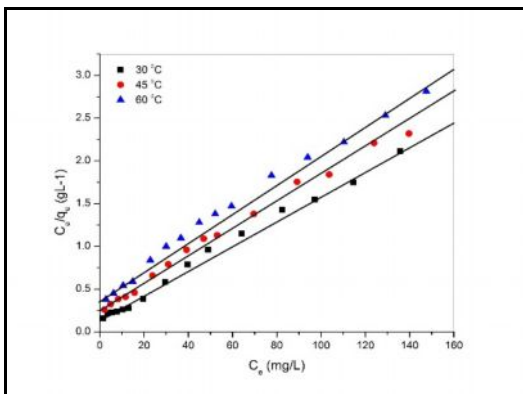


Fig. 3. Effect of Langmuir plot for the adsorption of Reactive blue 2 onto PWAC.

3.5.2. Freundlich isotherm

The empirical Freundlich isotherm is based on the equilibrium relationship between heterogeneous surfaces. This isotherm is derived from the assumption that the adsorption sites are distributed exponentially with respect to the heat of adsorption. The logarithmic linear form of Freundlich isotherm may be represented as follows [25].

$$\log q_e = \log K_F + \frac{1}{n} \log C_e$$

These slope values had indicated adsorption intensity n and the intercept values indicated an idea about adsorption capacity K_F . Where K_F (L/g) and $1/n$ are the Freundlich constants, indicating the sorption capacity and sorption intensity, respectively. The magnitude of K_F value decreased with increasing temperature, indicating that the adsorption process is exothermic in nature. The Freundlich adsorption isotherm was showed in Fig. 4.

The $1/n$ is a measure of adsorption intensity, also indicated that $0 < 1/n < 1$, indicating that Reactive blue 2 is favourably adsorbed by PWAC at all studied parameters. It was learnt that, If $n = 1$ then that the partition between the two phases was independent of the concentration. If the $1/n$ value is below one it indicates a normal adsorption. On the other hand $1/n$ being above one indicates cooperative adsorption [26].

The value of n greater than one confirmed that the activated carbon underwent a favorable for Freundlich isotherm.

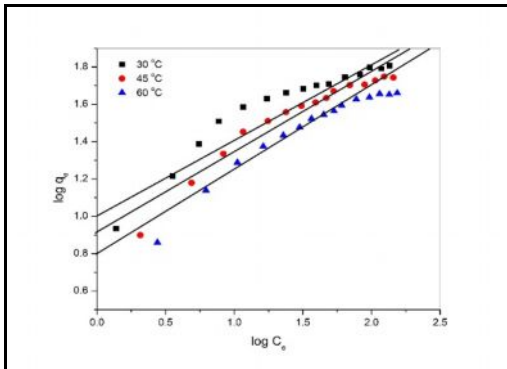


Fig.4. Effect of Freundlich plot for the adsorption of Reactive blue 2 onto PWAC.

3.5.3. Temkin isotherm

Temkin isotherm, assumes that the heat of adsorption decreases linearly with the coverage due to adsorbent-adsorbate interaction. The Temkin isotherm has generally been applied in the following linear form [27].

$$q_e = B \ln A + B \ln C_e$$

Where $B = RT/b$ constant related to heat of sorption. A (L/g) is Temkin isotherm constant, b (J/mol) is a constant related to heat of sorption, R is the gas constant (8.314 J/mol K) and T the absolute temperature (K). A plot of q_e versus $\ln C_e$ (Fig. 5) enables the determination of the isotherm constants A , b from the slope and intercept.

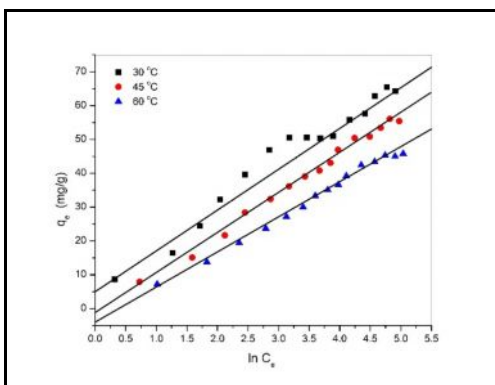


Fig. 5. Effect of Temkin plot for the adsorption of Reactive blue 2 onto PWAC.

The heat of dye adsorption (b) is directly related to coverage of dye onto PWAC due to adsorbent-adsorbate interaction. It was increased with increasing temperature from 208 to 265 J/mol, as listed in Table 1. This indicates that the heat of adsorption of Reactive blue 2 onto the surface of PWAC decreases with increasing temperature from 303 to 333 K and the sorption is exothermic.

3.5.4. Dubinin-Raduchkevich

Dubinin-Raduchkevich are used for estimating the mechanism of surface adsorption. Dubinin and Raduchkevich in 1947 proposed that the adsorption curve depends on the structure of the adsorbent pores [28]. The plot of $\ln q_e$ vs ϵ^2 at for Reactive blue 2 is presented in Fig. 6. The constant obtained for D-R isotherms are shown in Table 1. The mean adsorption energy (E) gives information about the chemical and physical nature of adsorption [29].

The linear form of the isotherm can be expressed as follows:

$$\ln q_e = \ln Q_D - B_D \epsilon^2$$

where Q_D is the theoretical maximum capacity (mol/g), B_D is the D-R model constant (mol²/kJ²), ϵ is the Polanyi potential and is equal to

$$\epsilon = RT \ln \left(1 + \frac{1}{C_e} \right)$$

The mean energy of sorption, E (kJ/mol), is calculated by the following equation

$$E = \frac{1}{\sqrt{2B_D}}$$

The Dubinin-Radushkevich, (DR) isotherm model is more general than the Langmuir isotherm as its deviations is not based on ideal assumptions such as equipotential of sorption sites, absence of steric hindrances between sorbed, incoming particles and surface homogeneity on microscopic level [30]. The estimated constant, Q_D gives an idea about the mean free energy which was valued as less than one. E is a parameter used in predicting the type of adsorption. An E value $< 8 \text{ kJmol}^{-1}$ is an indication of physisorption[25].

The DR Theoretical saturation capacity, Q_D and the Langmuir maximum adsorption capacity, Q_0 were both estimated as $Q_m = 67.79 \text{ mg g}^{-1}$ and $Q_D = 46.90 \text{ mgg}^{-1}$. Q_D is always lesser than the maximum adsorption capacity as the case was made evidence in this research.

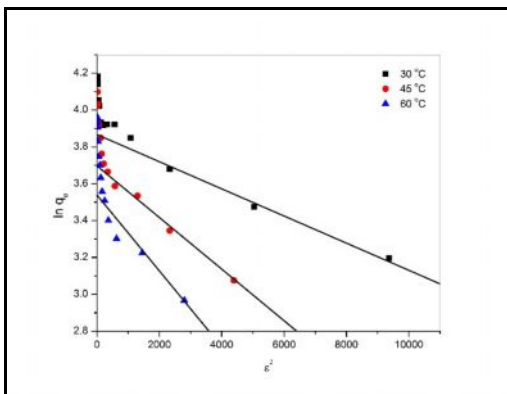


Fig. 6. Effect of DR plot for the adsorption of Reactive blue 2 onto PWAC.

3.5.5. Halsey adsorption isotherm

The Halsey adsorption isotherm can be given as [32].

$$q_e = \exp \left[\frac{\ln K_H - \ln C_e}{n_H} \right]$$

and a linear form of the isotherm can be expressed as follows

$$\ln q_e = \frac{\ln K_H}{n_H} - \frac{\ln C_e}{n_H}$$

This equation is suitable for multilayer adsorption and the fitting of the experimental data to this equation attest to the heteroporous nature of adsorbent where $k(\text{mg/L})$ and n are the Halsey isotherm constants. The n values are represented in table 1. The plot $\ln q_e$ vs $\ln C_e$ was showed in Fig. 7.

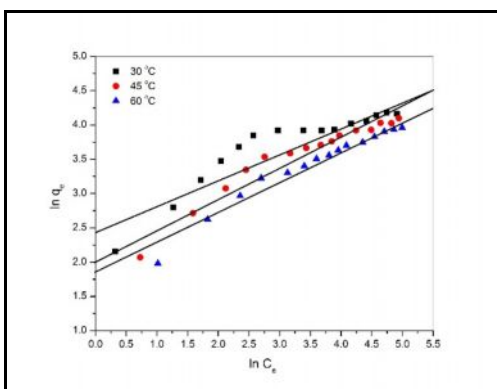


Fig. 7. Effect of Halsey isotherm plot for the adsorption of Reactive blue 2 onto PWAC.

3.5.6. Jovanovic adsorption isotherm

The model of an adsorption surface considered by Jovanovic [33] is essentially the same as that considered by Langmuir. The Jovanovic model leads to the following relationship [22].

$$q_e = q_{\max}(1 - e^{-K_J C_e})$$

The linear form of the isotherm can be expressed as follows:

$$\ln q_e = \ln q_{\max} - K_J C_e$$

The SSE and chi square values for the Jovanovic model were slightly higher for Langmuir model. But RMSE value is higher than that of all other models indicate Jovanovic did not suitable for the adsorption process. Fig.8 represents the Jovanovic adsorption isotherm. Where $K_J(L/g)$ is a parameter. K_J and q_{\max} (mg/g) is the maximum Reactive blue 2uptake is represented in table 1 at different temperatures.

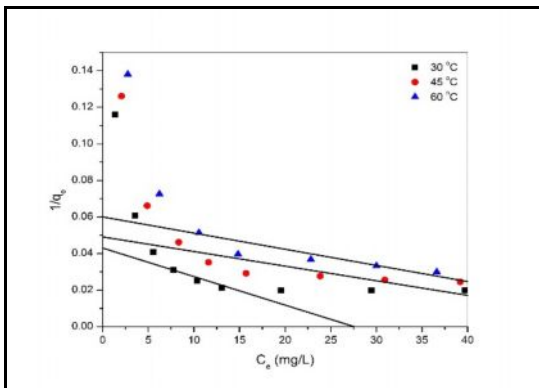


Fig. 8. Effect of Jovanovic isotherm plot for the adsorption of Reactive blue 2 onto PWAC.

3.5.7. Error analysis

The error analysis values for Langmuir, Freundlich, Temkin, D-R, Halsey and Jovanovic isotherm models at 303, 313 and 333K are presented in Table 1. it would seem (that), it can be concluded that the most applicable isotherm to relate Acid red 114-PWAC adsorption system is Langmuir isotherm. The values of regression coefficients, R^2 and the non-linear error functions (SSE, RMSE and chi-square) are in accordance to one another. despite the fact that the linear regression coefficients, R^2 of the Freundlich are less than 0.99 at 303,313 and 323K. Thus, Langmuir is still considerable to describe this adsorption system. The D-R is the least applicable isotherm as the linear regression coefficients, R^2 were less than 0.7 and the non-linear error functions (SSE and chi-square) are higher in value at all temperature range. The SSE value more than 5% is not recommended due to intolerant margin of deviation between the experimental data and the model calculated data. The Halsey and Jovanovic isotherm regression coefficients, R^2 were less than 0.8 and the non-linear error functions (SSE and chi-square) are higher in value at all temperature indicates the non-suitability of adsorption. Langmuir models show a high degree of correlation with low root mean square error (RMSE), SSE and chi-square values.

Model	Isotherm Constants	Reactive dye		
		30 °C	45 °C	60 °C
Langmuir	$Q_0(\text{mg g}^{-1})$	67.79	61.59	51.65
	$K_L(\text{L mg}^{-1})$	0.0896	0.0614	0.0524
	R^2	0.9965	0.9976	0.9985
	SSE	0.0211	0.0187	0.0181
	χ^2	0.0309	0.0234	0.0193
	RMSE	0.1371	0.1181	0.1301
Freundlich	$1/n$	0.3865	0.4239	0.4296
	$K_f(\text{mg g}^{-1})(\text{L mg}^{-1})^{1/n}$	11.5053	8.1613	6.3410
	R^2	0.8938	0.9291	0.9399
	SSE	0.0894	0.0566	0.0430
	χ^2	0.0702	0.0462	0.0369
	RMSE	0.2755	0.2199	0.1900
Temkin	$\beta_T(\text{KJ mol}^{-1})$	12.2696	11.8922	10.2769
	$\alpha_T(\text{L mg}^{-1})$	1.5049	0.8484	0.6624
	b	208.7046	222.3182	265.3515
	R^2	0.9855	0.9933	0.9929
	SSE	59.2728	20.8845	14.6062
	χ^2	2.0596	0.8218	0.5264
	RMSE	7.2080	4.3688	3.7145
Halsey	$K_h(\text{mg g}^{-1})$	555.5709	141.5419	73.6934
	n	2.5872	2.3590	2.3280
	R^2	0.8938	0.9291	0.9399
	SSE	2.8347	1.5529	1.1609
	χ^2	2.1547	0.7858	0.4966
	RMSE	1.6434	1.1532	1.0291
D-R	$K\text{-DR}(\text{mol}^2 \text{KJ}^{-2})$	1.860E-05	3.441E-05	5.314E-05
	$Q_m(\text{mg g}^{-1})$	46.90	40.96	34.67
	R^2	0.7409	0.7337	0.7426
	SSE	1.1559	1.1284	0.9755
	χ^2	0.3592	0.3555	0.3171
	RMSE	0.9557	0.9813	0.9372
	E			
Jovanovic	q_{\max}	1.0466	1.0543	1.0632
	K_J	0.0090	0.0089	0.0081
	R^2	0.4902	0.5430	0.5642
	SSE	0.0180	0.0215	0.0268
	χ^2	0.1423	0.1567	0.1759
	RMSE	838.2393	797.2756	752.1067

3.6. Adsorption Kinetics

Kinetic models have been proposed to determine the mechanism of the adsorption process which provides useful data to improve the efficiency of the adsorption and feasibility of process scale-up[34]. Physical and chemical properties of the adsorbents as well as mass transfer processes are some influential parameters to determine the adsorption mechanism [35]. The analysis of experimental data at various times makes it possible to calculate the kinetic parameters and to take some information for designing and modeling of the adsorption processes. To understand the adsorption mechanism of PWAC for acid red 114, the adsorption kinetics were investigated using pseudo first-order, pseudo-second order the Elovich and Intraparticle diffusion kinetic equation models.

3.6.1. Pseudo first-order kinetic model

The pseudo-first-order kinetic model [36] can be expressed as

$$\log[(q_e - q_t)] = \log q_e - \left(\frac{K_L}{2.303}\right)t$$

According to this equation, a plot of $\log (q_e - q_t)$ versus time should be linear. However, in our experiments, q_e remains unknown due to slow adsorption process and therefore, linearity in the plots of $\log(q_e - q_t)$ versus time (t) could not be observed. It has been observed in many cases that the first order equation of Lagergren does not fit well for the whole range of contact time and is generally applicable over the initial stage of adsorption process[37].

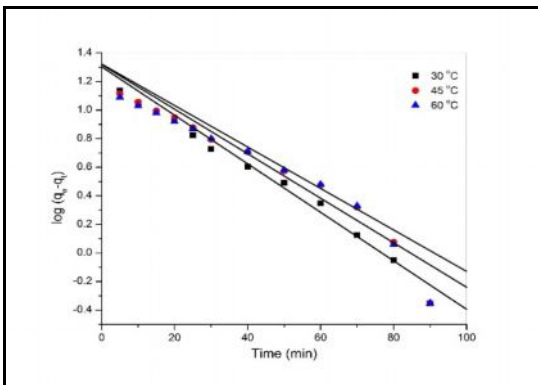


Fig. 9. Effect of Pseudo first order plot for the adsorption of Acid 114 onto PWAC

Fig. 9 shows a plot of linearization form of pseudo first-order model at different temperatures were studied. The slopes and intercepts of plots of $\log (q_e - q_t)$ versus t were used to determine the pseudo first-order constant k_1 and equilibrium adsorption density q_e . However, the experimental data deviated considerably from the theoretical data. A comparison of the results with the correlation coefficients is shown in Table 3. The correlation coefficients for the pseudo first order kinetic model obtained at all the studied temperatures were less than 0.98. Also the theoretical q_e values found from the pseudo first-order kinetic model did not give reasonable values. This result suggests that the adsorption system is not suitable for pseudo first-order reaction[38].

3.6.2. Pseudo Second Order Kinetic Model

To describe the dye adsorption, the modified pseudo second order kinetic equation is expressed as[39]

$$\frac{t}{q_t} = \frac{t}{K_2 q_e^2} + \frac{1}{q_e} t$$

where K_2 is the rate constant of pseudo-second-order model (g/mg.min) and q_e is derived from the linear plot of t/q_t versus t. The second-order rate constant was used to calculate the initial adsorption rate (h) given by the equation

$$h = K_2 q_e^2$$

The rate constants and correlation coefficients (R^2) of the kinetic models are listed in table 1.

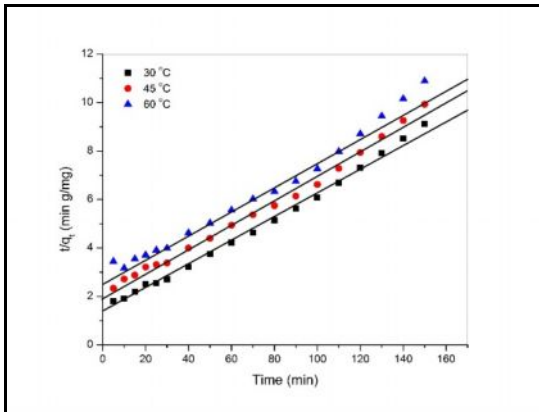


Fig. 10. Effect of Pseudo second order plot for the adsorption of Acid 114 onto PWAC

From the results, pseudo second-order kinetic model gave $R^2 > 0.99$ for all temperatures. The values of the rate constants decreased with increasing temperature. The q_e values calculated from the linear plot of the pseudo-second-order kinetic model were also found to be in agreement with experimental q_e values (table 2). Since pseudo-second-order kinetic model fitted better with this system than the pseudo first-order kinetic model, coupled with the high agreement between its calculated and experimental q_e values it can be suggested that the adsorption was controlled by physisorption. This process involves valence forces through exchange of electrons between adsorbate and adsorbent. Also the decrease in rate constant K_2 as the temperature increases reveals the fact that it is faster for the adsorption system with Reactive blue 2 to reach equilibrium.

3.6.3. Elovich model

We can write the Elovich kinetic model as [40]

$$\frac{dQ}{dt} = \alpha \exp(-\beta Q)$$

In this model, α is known initially as the rate of adsorption with the unit of $\text{mg} \cdot \text{g}^{-1} \cdot \text{min}^{-1}$. β is known as coefficient of desorption as $\text{g} \cdot \text{mg}^{-1}$. We can rewrite the Elovich kinetic model equation, with assumptions of

$\alpha\beta t \gg 1$ and by using two boundary conditions. These conditions are $Q = 0$ for time of $t = 0$ and $Q = Q_t$ for time

of $t = t$. With these assumptions, the Elovich model equation can be written as

$$Q_t = \beta \ln \alpha \beta + \frac{1}{\beta} \ln(t)$$

If Reactive blue 2 adsorption with using PWAC obeys the Elovich kinetic model, Q_t vs $\ln t$ must give a line with a slope of values of $(1/\beta)$; $\ln(\alpha\beta)$ can be found as the intercept. This procedure has been applied in Fig. 11.

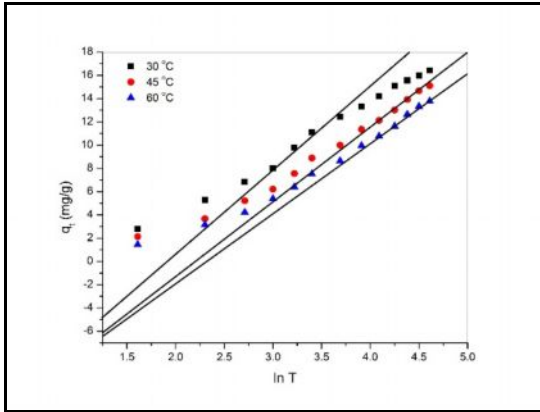


Fig. 11. Effect of Elovich plot for the adsorption of Reactive blue 2 onto PWAC

The correlation coefficient R^2 showed that the pseudo-second-order model, indicative of a physisorption mechanism, fit the experimental data slightly better than the Elovich and the pseudo-first order models. In other words, the adsorption of Reactive blue 2 could be approximated more favorably by the pseudo-second-order kinetic model.

Table 2 lists also the kinetic constants obtained from the Elovich equation. On increasing the temperature from 30 to 60 °C, the values of β have slight significant variation. However, the constant α decreased as the temperature increased. This behavior suggests that more than one mechanism controls the adsorption process [41]. For the Elovich model, the correlation coefficients (R^2) are relatively high (>0.96). It indicates that the Elovich model can also be suitable for describing the adsorption kinetic of Reactive blue 2 onto PWAC.

The Elovich equation provides the best correlation for all of the sorption process, whereas the pseudo second-order equation also fits the experimental data well. This suggests that the sorption systems studied belong to both the Elovich equation and the pseudo second-order kinetic model with experimental data. The adsorption system obeys the pseudo second-order kinetic model for the entire adsorption period and thus supports the assumption behind the model that the adsorption is due to physisorption.

3.6.4. Intraparticle Diffusion Model

The most-widely applied intraparticle diffusion equation for sorption which describes the diffusion mechanism and rate controlling steps given by Weber and Morris [42] is

$$q_t = k_{id}t^{1/2} + C$$

where, q_t is the fraction dye uptake (mg/g) at time t , k_{id} is the intra-particle diffusion rate constant (mg/g min^{1/2}) and C is the intercept (mg/g). The plot of q_t versus $t^{1/2}$ will give k_{id} as slope, C represents the effect of boundary layer thickness between solute and adsorbent. Minimum is the intercept length, adsorption is less boundary layer controlled.

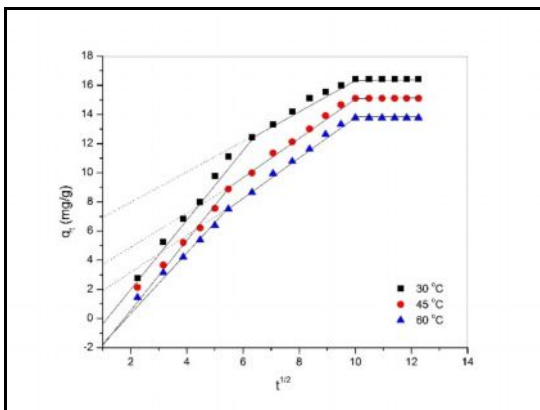


Fig. 12. Effect of Intraparticle plot for the adsorption of Reactive blue 2 onto PWAC.

The correlation coefficient (R^2) values of intraparticle diffusion models were higher and also give the intercept value. The value of intercept indicates that the lines were not passing through origin, signifying that adsorption involved intraparticle diffusion, nevertheless that was not the only rate-controlling step [43], and thus some other adsorption process affect the intraparticle diffusion. This was due to the surface adsorption or boundary layer adsorption. Almost all the correlation coefficient (R^2) value was greater than 0.98 for 30 to 60 °C. So the intraparticle diffusion takes place along with the boundary layer effect[44].

3.7. Adsorption Thermodynamics

The standard Gibbs free energy ΔG° (kJ mol⁻¹), standard enthalpy change ΔH° (kJ mol⁻¹), and standard entropy change ΔS° (J mol⁻¹K⁻¹) were calculated using the following equations:

$$\Delta G^\circ = -RT \ln K_0$$

$$\ln K_0 = \frac{\Delta S^\circ}{R} - \frac{\Delta H^\circ}{RT}$$

Where R is the universal gas constant (8.314 J mol⁻¹ K⁻¹), T is the temperature in Kelvin and K_0 is the equilibrium constant.

The plot of $\ln K_0$ vs. $1/T$ was linear and the values of ΔH° and ΔS° were resolved from the slope and intercept. The values of these parameters are show in table 5. The value of enthalpy change ΔH° (-20.60KJmol⁻¹) is negative indicating the adsorption is exothermic process.

The negative values of ΔG° at all temperatures (30, 45 and 60 °C, respectively) verified the thermodynamic feasibility and spontaneity of the adsorption process. The negative value of ΔS° (-55.31 J. mol⁻¹K⁻¹) suggests that the disorder at the solid–liquid interface decreased during dye adsorption and that no significant changes occurred in the internal structure of the adsorbents upon adsorption [45]. When the value of ΔS° is higher than -10 kJ mol⁻¹, a dissociative mechanism controls the adsorption process [46-48]. The values of ΔG° at all temperatures studies as presented in table 2 were indications that the sorption process was physisorption since the values are between-20 to 0 kJ mol⁻¹ [49].

Kinetic Model		Temperature		
		30 °C	45 °C	60 °C
Pseudo-first Order	K_1 (min ⁻¹)	-0.0335	-0.0336	-0.0372
	R^2	0.9760	0.9754	0.8915
	SSE	3.1023	3.1797	3.6641
	χ^2	2.7754	4.2998	2.8896
	RMSE	1.7449	1.7665	1.9043
Pseudo-second Order	K_2 (g/mg min)	0.0017	0.0012	0.0010
	h	0.7056	0.5072	0.3966
	q_e	16.44	15.11	13.78
	R^2	0.9956	0.9961	0.9907
	SSE	0.4183	1.0570	0.9890
	χ^2	0.0800	0.1902	0.1372
	RMSE	0.6369	1.1011	0.9869
Elovich	α	1.5069	1.1153	0.9114
	β	0.2227	0.2240	0.2410
	R^2	0.9828	0.9751	0.9676
	SSE	5.8826	8.5167	6.4924
	χ^2	0.5141	1.3267	1.6274
	RMSE	2.5640	3.2405	2.6466
IPD	K_{id}	1.8971	1.8718	1.6292
	R^2	0.9859	0.9265	0.9974
	SSE	28.6374	25.1262	14.1283
	χ^2	3.7825	3.1541	1.8981
	RMSE	5.7855	5.4072	4.0347

Thermodynamic parameters for the adsorption of Reactive blue 2 onto PWAC

Dye	T(K)	ΔG° (kJ/mol)	ΔH° (kJ/mol)	ΔS° (kJ/mol K)	Ea(kJ/mol)
Reactive blue 2	303	-3.8576	-20.6050	-55.3168	2.8481
	318	-2.9841			
	333	-2.2010			

Conclusions

In this present study, plastics waste was converted to activated carbon as low cost sorbent used for the sorption of reactive dye from textile industrial effluents. We could conclude that the analysis by SEM and XRD showed that the adsorbent material has a micro porous and crystalline structure. Equilibrium data fitted very well in the Langmuir isotherm equation, confirming the monolayer adsorption capacity of Reactive blue 2 onto PWAC with activation energy a monolayer adsorption capacity of 68.21 mg/g. The non-linear analysis shows the adsorption process was strongly followed Langmuir adsorption isotherm model. The rate of adsorption was decrease with increase in temperatures of the reactive blue 2 dye onto PWAC adsorption system. The kinetic of adsorption of Reactive blue 2 obeyed well with the pseudo-second-order model. The results of the intraparticle diffusion model suggest that the diffusion was not found the rate determining step. Thermodynamic study reveals the spontaneous and exothermic nature of adsorption process owing to negative values of free energy and enthalpy change with activation energy $E_a = 2.8481$ kJ/mol. The adsorption technique is favourable for the physisorption mechanism. The validity of the kinetic models analyzed using SSE, Chi square and RMSE methods find the adsorption was best fitted by pseudo second order kinetic model.

References

1. A.E. Ghaly, R. Ananthashankar, M. Alhattab, V.V. Ramakrishnan., Production, Characterization and Treatment of Textile Effluents: A Critical Review, *J ChemEng Process Technol* 2014, 5:1)
2. S.Chowdhury, R.Mishra, P. Sha, P. Kushwa, adsorption, thermodynamics, kinetics and isosteric heat of adsorption of malachite green onto chemically modified rice husk. *Desalination*. 265 (2011) 159-168)
3. D. Peterson, *Colorants and Auxiliaries: Organic Chemistry and Application Properties*, in: J. Shore (Ed.), BTTG- Shirley, Manchester 1990, pp. 32–72).
4. MohdAzmeer Ahmad, NurAzreen Ahmad Puad, Olugbenga Solomon Bello, Kinetic, equilibrium and thermodynamic studies of synthetic dye removal using pomegranate peel activated carbon prepared by microwave-induced KOH activation, *Water Resources and Industry* 6 (2014) 18–35.
5. *Plastics-The Facts 2013: An Analysis of European Latest Plastics Production, Demand and Waste Data*; Plastics Europe, Brussels, 2013.
6. Neha Patni, Pallav Shah, Shruti Agarwal, and PiyushSinghal, Alternate Strategies for Conversion of Waste Plastic to Fuels *International Scholarly Research Notices*, Volume 2013 (2013), Article ID 902053).
7. P. Senthil Kumar M. Bharathikumar, C. Prabhakaran, S.Vijayan, K. Ramakrishnan, Conversion of waste plastics into low-emissive hydrocarbon fuels through catalytic depolymerization in a new laboratory scale batch reactor, *Int J Energy Environ Eng*. 2015).
8. D. P. Serrano, J. Aguado, J. M. Escola, Developing advanced catalysts for the conversion of polyolefinic waste plastics into fuels and chemicals. *ACS Catal.* 2 (2012) 1924–1941.
9. C. Dorado, C. A. Mullen, A. A. Boateng, H-ZSM5 catalyzed co-pyrolysis of biomass and plastics. *ACS Sustainable Chem. Eng.* 2 (2014) 301–311.
10. P. T. Williams, E. Slaney, Analysis of products from the pyrolysis and liquefaction of single plastics and waste plastic mixtures. *Resour. Conserv. Recycl.* 51 (2007) 754–769.
11. P. Balakrishna Murthy, A. Sairam Kishore and P. Surekha, Acute Toxicological Effects of Multi-Walled Carbon Nanotubes (MWCNT) *Nanotechnology and Nanomaterials Carbon Nanotubes - Growth and Applications* Edited by Dr. Mohammad Naraghi, (2011).
12. H. Guedidi, L. Reinert, Y. Soneda, N. Bellakhal, L. Duclaux. Adsorption of ibuprofen from aqueous solution on chemically surface-modified activated carbon cloths, *Arab. J. Chem.* (2014) In press.

13. A.R. Binupriya, M. Sathishkumar, S.H. Jung, S.H. Song, S.I. Yun, A novel method in utilization of Bokbunja seed wastes from wineries in liquid-phase sequestration of Reactive Blue 4, *Int. J. Environ. Res.* 3 (2009) 1-12.
14. H. Deng, G. Zhang, X. Xu, G. Tao, J. Dai, Optimization of preparation of activated carbon from cotton stalk by microwave assisted phosphoric acid-chemical activation, *J Hazard Mater.* 182 (2010) 217-224.
15. T. Yang, A.C. Lua, Characteristics of activated carbons prepared from pistachio-nut shells by physical activation. *J. Colloid Interface Sci.* 267 (2003) 408–417.
16. S. Lu, D. Cao, X. Xu, H. Wang, Y. Xiang, Study of carbon black supported amorphous Ni–B nanocatalyst for hydrazine electro-oxidation in alkaline media, *RSC Adv.* 4 (2014) 26940–26945.
17. B.R. Venkatraman. U. Gayathri, S. Elavarasi, S. Arivoli, Removal of Rhodamine B dye from aqueous solution using the acid activated Cynodondactylon carbon, *Der. Chemica. Sinica*, 3 (2012) 99-113.
18. Z. Xie, W. Guan, F. Ji, Z. Song, Y. Zhao, Production of biologically activated carbon from orange peel and landfill leachate subsequent treatment technology, *J. Chem.* (2014) 1-9.
19. M. F. Elkady, M. M. Hussein, M. M. Salama, Synthesis and characterization of nano-activated carbon from el maghara coal, Sinai, Egypt to be utilized for wastewater Purification, *Am. J. Appl. Chem.* 3 (2015) 1-7.
20. Wengui Zhang, Dinghua Yu, XiaojunJia, He Huang, Efficient dehydration of bio-based 2,3-butanediol to butanone over boric acid modified HZSM-5 zeolites, *Green Chem.* 14 (2012) 3441–3450.
21. IsakRajjak Shaikh, Rafique Ahmed Shaikh, Alamgir Abdulla Shaikh, Javeed Ahmad War, Shankar PoshettiHangirgekar, Ahmad LalahmadShaikh, ParveenRajjak Shaikh, RafikRajjak Shaikh, H-ZSM-5 Zeolite Synthesis by Sourcing Silica from the Wheat Husk Ash: Characterization and Application as a Versatile Heterogeneous Catalyst in Organic Transformations including Some Multicomponent Reactions, *Journal of Catalysts*, 1 (2015) 1-14.
22. A. Khaled, A. El Nemr, A. El-Sikaily, O. Abdelwahab, Treatment of artificial textile dye effluent containing Direct Yellow 12 by orange peel carbon, *Desalination.* 238 (2009) 210-232.
23. I. Langmuir, The constitution and fundamental properties of solids and liquids, *J. Am. Chem. Soc.* 38 (1916) 2221–2295.
24. B. Abbad, A. Lounis, K. Taibi, M. Azzaz, Removal of methylene blue from coloured effluents by adsorption onto ZnAPSO-34 nanoporous material, *J. Mater. Sci. Eng.* 2 (2013) 1-6.
25. H.M.F. Freundlich, Over the adsorption in solution, *J. Phys. Chem.* 57 (1906) 385–471.
26. P.S. Syed Shabudeen, Adopting response surface methodology to design an experiment in studying the removal of dye by utilizing solid agricultural waste activated carbon, *Int. J. Sci. Technol.* 1 (2011) 118-127.
27. M.I. Tempkin, V. Pyzhev, Kinetics of ammonia synthesis on promoted iron catalyst, *Acta Phys. Chim. USSR.* 12 (1940) 327–356.
28. M.M. Dubinin, E.D. Zaverina, L.V. Radushkevich, Sorption and structure of active carbons, I. Adsorption of organic vapors. *Zhurnal Fizicheskoi Khimii.* 21 (1947) 1351–1362.
29. W. Rieman, H. Walton, Ion Exchange in Analytical Chemistry, International Series of Monographs in Analytical Chemistry, Pergamon Press, Oxford, 1970.
30. J. Monika, V. Garg, K. Kadirvelu, Chromium (VI) removal from aqueous solution, using sunflower stem waste, *J. Hazard. Mater.* 162 (2009) 365–372.
31. A.U. Itodo, H.U. Itodo, Utilizing D-R and Temkin isotherms with GCMS external standard technique in forecasting liquid phase herbicide sorption energies. *Electronic J. Environ. Agri. Food Chem.* 9 (2010) 1792-1802.
32. C.A. Basar, Applicability of the various adsorption models of three dyes adsorption onto activated carbon prepared waste apricot. *J. Hazard. Mater.* 135 B (2006) 232-241.
33. Y.S. Ho, J.F. Porter, G. McKay, Equilibrium isotherms studies for the sorption of divalent metal ions onto peat: copper, nickel and lead single component systems, *Water, Air and Soil Pollut.* 141 (2002) 1-33.
34. S. Eftekhari, A. Habibi-Yangjeh, S. Sohrabnezhad, Application of AIMCM-41 for competitive adsorption of methylene blue and Rhodamine B: Thermodynamic and kinetic studies, *J. Hazard. Mater.* 178 (2010) 349-355.
35. M. Mohammadi, A.J. Hassani, A.R. Mohamed, G.D. Najafpour. Removal of Rhodamine B from aqueous solution using palm shell-based activated carbon: adsorption and kinetic studies, *J. Chem. Eng. Data.* 55 (2010) 5777–5785.

36. S. Lagergren. About the theory of so-called adsorption of soluble substances, *Kungliga Sven. Vetensk. Handl.* 24 (1898) 1–39.
37. S. Chandravanshi, S.K. Upadhyay, Kinetic, equilibrium and thermodynamic studies of adsorption of terminaliaarjuna natural dye on cotton in presence of cationic surfactant, *Int. J. Fiber. Text. Res.* 4 (2014) 20-26.
38. M. Al-Meshragi, H.G. Ibrahim, M.M. Aboabboud, Equilibrium and kinetics of chromium adsorption on cement kiln dust. *Proc. World Congress Eng. Computer Sci.*, San Francisco, USA, 2008.
39. D. Sun, X. Zhang, Y. Wu, X. Liu, Adsorption of anionic dyes from aqueous solution on fly ash, *J. Hazard. Mater.* 181 (2010) 335–342.
40. F.C. Wu, R.L. Tseng, R.S. Juang, Characteristics of Elovich equation used for the analysis of adsorption kinetics in dye-chitosan systems, *Chem. Eng. J.* 150 (2009) 366–373.
41. M.A. Ahmad, N.A.A. Puad, O.S. Bello. Kinetic, equilibrium and thermodynamic studies of synthetic dye removal using pomegranate peel activated carbon prepared by microwave-induced KOH activation, *Water Resour. Ind.* 6 (2014) 18–35.
42. AamnaBalouch, MazharKolachi, Farah NazTalpur, Humaira Khan, Muhammad I. Bhanger, Sorption Kinetics, Isotherm and Thermodynamic Modeling of Defluoridation of Ground Water Using Natural Adsorbents, *Sci. Res.* 4 (2013) 221-228
43. H. El-Boujaady, M. Mourabet, M. Bennani-Ziatni, A. Taitai, Adsorption/desorption of Direct Yellow 28 on apatitic phosphate: Mechanism, kinetic and thermodynamic studies, *J. Asso. Arab Uni. Basic Appl. Sci.* 16 (2014) 64–73.
44. M. Thilagavathi, S. Arivoli, V. Vijayakumaran. Kinetic and thermodynamic studies on the adsorption behavior of Rhodamine B dye using Prosopis Juliflora bark carbon, *Sci. J. Eng. Tech.* 2 (2014) 258-263.
45. A. Roy, B. Adhikari, S.B. Majumder, Equilibrium, Kinetic, and Thermodynamic studies of azo dye adsorption from aqueous solution by chemically modified lignocellulosic jute fiber. *Ind. Eng. Chem. Res.* 52 (2013) 6502–6512.
46. B.W. Hu, W. Cheng, H. Zhang, S.T. Yang, Solution chemistry effects on sorption behavior of radionuclide $^{63}\text{Ni}(\text{II})$ in illite-water suspensions, *J. Nucl. Mater.* 406 (2010) 263–270.
47. S. Yang, D. Zhao, H. Zhang, S. Lu, L. Chen, X. Yu. Impact of environmental conditions on the sorption behavior of $\text{Pb}(\text{II})$ in Na-bentonite suspensions, *J. Hazard. Mater.* 183 (2010) 632–640.
48. S. Yang, Z. Guo, G. Sheng, X. Wang, Investigation of the sequestration mechanisms of $\text{Cd}(\text{II})$ and 1-naphthol on discharged multi-walled carbon nanotubes in aqueous environment, *Sci. Total. Environ.* 420 (2012) 214–221.
49. O. Alao, J.A. Chijioke, O. Ayeni, Kinetics, equilibrium and thermodynamic studies of the adsorption of Zinc (II) ions on Carica papaya root powder, *Res. J. Chem. Sci.* 4 (2014) 32-38.
